

# Photoluminescence Study of B-Trions in MoS<sub>2</sub> Monolayers with High Density of Defects

Reelika Kaupmees, Hannu-Pekka Komsa, and Jüri Krustok\*

Photoluminescence spectroscopy has been used to investigate the details of *B* band emission from single-layer MoS<sub>2</sub> samples grown by chemical vapor deposition. The evolution of the peak shape upon variable excitation power is well described by a combination of exciton and trion contributions, from which *B* trion binding energy of 18 meV has been extracted. It has been suggested that the absence of accompanying *A* trion emission in our samples, as well as the enhanced intensity of the *B* band, can be ascribed to a fast non-radiative recombination channel arising from the large defect density in our samples. It has been found that band-selective recombination channels or formation of dark/bright trions are possible microscopic scenarios for our observations.

## 1. Introduction

The appearance of 2D atomic crystals with various optical and electrical properties has opened up new routes for electronic and optoelectronic device fabrication based on atomically thin layers.<sup>[1,2]</sup> Among them, monolayers of transition metal dichalcogenides (TMDs), such as MoSe<sub>2</sub>, WSe<sub>2</sub>, and MoS<sub>2</sub>, are the most attractive having well-defined semiconductor properties.<sup>[3]</sup> MoS<sub>2</sub> is the most studied TMD atomic crystal, where an atomic plane of Mo atoms is found between two layers of S atoms in a trigonal prismatic structure forming a so-called monolayer.<sup>[4]</sup> In multilayer arrangements, monolayers are stacked together with weak van der Waals interactions between S atoms. While first MoS<sub>2</sub> monolayers were obtained by mechanical exfoliation,<sup>[1]</sup> other methods are proved to be more promising to produce large area and high quality 2D materials to

enable their industrialization. Among them, the chemical vapor deposition (CVD) method is the most popular one and has been successfully demonstrated in synthesis of MoS<sub>2</sub> monolayers and other 2D materials.<sup>[5–12]</sup>

The band structure of MoS<sub>2</sub> converts from an indirect bandgap to a direct one when decreasing its thickness from bulk to a single layer. As a result the photoluminescence (PL) intensity increases remarkably and two PL bands emerge at about 1.8 and 1.95 eV at room temperature.<sup>[13–15]</sup> These bands are called *A* and *B* band, respectively, and they correspond to the direct excitonic transitions at the *K* point in the Brillouin zone, where the *B*

band is related to the spin-orbit split lower valence band. The value of spin-orbit splitting of the valence band in MoS<sub>2</sub> monolayers is  $\Delta E_{\text{SO}} = 148 \text{ meV}$ ,<sup>[16]</sup> while the splitting of the conduction band is very small and does not exceed 5 meV. The actual peak position of *A* and *B* bands depends on type of the substrate and on quality of monolayers. It has been shown that monolayers grown by CVD on SiO<sub>2</sub>/Si substrates usually show PL bands at lower energy than in exfoliated monolayers<sup>[17,18]</sup> and this is caused by intrinsic tensile strain in MoS<sub>2</sub> monolayer.<sup>[19,20]</sup> The strain and the presence of lattice defects affect not only PL bands, but also the position of Raman peaks of monolayer.<sup>[20–23]</sup> It has been shown that the *A* band at room temperature is often a sum of neutral (*A*<sup>0</sup>) and charged (*A*<sup>−</sup>) exciton emissions.<sup>[24–27]</sup> The charged exciton is called trion and, in principle, it could be either negative (*A*<sup>−</sup>) or positive (*A*<sup>+</sup>) depending on the type of majority carriers. Theoretical calculations show that the same double peak structure is expected also for the *B* band.<sup>[28–30]</sup> Experimentally the *B*<sup>−</sup> trion has been recently observed by reflectance contrast measurements in WSe<sub>2</sub> and MoSe<sub>2</sub>,<sup>[31]</sup> but attempts to detect the existence of *B*<sup>−</sup> (or *B*<sup>+</sup>) trion by PL have not been successful.

In this work, the photoluminescence properties of CVD grown single-layer MoS<sub>2</sub> are investigated by using variable excitation power in order to detect a presence of the *B* trion.


## 2. Experimental Section

MoS<sub>2</sub> monolayers were grown by a CVD method on a Si substrate with a 275 nm thick SiO<sub>2</sub> layer and using MoO<sub>3</sub> and S precursors. For the CVD process, a two-zone furnace was used with S zone at 200 °C and MoO<sub>3</sub> zone at 790 °C. N<sub>2</sub> was used as a carrier gas with a gas flow of 100 sccm. The Si/SiO<sub>2</sub> substrate

R. Kaupmees, Prof. J. Krustok  
Department of Materials and Environmental Technology  
Tallinn University of Technology  
Ehitajate tee 5, 19086 Tallinn, Estonia  
E-mail: juri.krustok@ttu.ee

Dr. H.-P. Komsa  
Department of Applied Physics  
Aalto University  
P.O. Box 11100, 00076 Aalto, Finland

Prof. J. Krustok  
Division of Physics  
Tallinn University of Technology  
Ehitajate tee 5, 19086 Tallinn, Estonia

 The ORCID identification number(s) for the author(s) of this article can be found under <https://doi.org/10.1002/pssb.201800384>.

DOI: 10.1002/pssb.201800384

was positioned face-down at about 2 cm from a MoO<sub>3</sub> precursor. This growth process produced uniform MoS<sub>2</sub> domains and the size of these areas ranges from several tens to more than hundred micrometers. Raman and PL-unpolarized measurements were carried out using a Horiba LabRAM HR800 Micro-Raman system equipped with a multichannel CCD detection system in the backscattering configuration with a spectral resolution better than 1 cm<sup>-1</sup>. An Nd-YAG laser (wavelength 532 nm) was used for excitation. The laser spot size was about 2 μm in diameter. The scanning electron microscope (SEM) HR-SEM Zeiss Merlin was used to study the morphology of monolayers.

### 3. Results and Discussion

**Figure 1** shows a SEM picture of the monolayer and the Raman spectrum from the CVD-grown MoS<sub>2</sub>. The Raman peaks associated with MoS<sub>2</sub>, namely, the in-plane mode *E'* (381.7 cm<sup>-1</sup>) and the out-of-plane mode *A'*<sub>1</sub> (405.0 cm<sup>-1</sup>) are clearly seen in **Figure 1**.<sup>[33,34]</sup> The separation between these peaks is  $\Delta = 23.3 \text{ cm}^{-1}$  and this value is higher than usually observed separation in high quality monolayers ( $\Delta \approx 19 \text{ cm}^{-1}$ <sup>[34]</sup>). Vertical-dashed lines in **Figure 1** mark the peak positions of high quality exfoliated monolayer and, with respect to these lines, our CVD-grown MoS<sub>2</sub> has peaks that are either softened (*E'*) or stiffened (*A'*<sub>1</sub>), which can be attributed to the presence of substrate-induced tensile strain and charge doping.<sup>[19,35]</sup> The origin of tensile strain in CVD-grown MoS<sub>2</sub> layers has been attributed to the mismatch of the thermal expansion coefficient between the layer and a SiO<sub>2</sub>/Si substrate<sup>[19]</sup> or/and to the surface roughness.<sup>[6,36]</sup> It is known that the lattice tensile strain affects predominantly the in-plane vibration mode *E'* while the *A'*<sub>1</sub> mode is relatively unaffected:  $-2.1 \text{ cm}^{-1}$  per % strain and  $-0.4 \text{ cm}^{-1}$  per % strain, respectively.<sup>[22]</sup> According to these estimations our MoS<sub>2</sub> monolayer seems to have a tensile strain in the range of 1%. However, the shift of *E'* mode can be also related to high defect

(mostly sulfur vacancies) concentration as was shown in ref. [21]. The blue shift of the *A'*<sub>1</sub> peak is believed to be a result of hole doping, because, due to the strong interaction between *A'*<sub>1</sub> phonon and electrons, the *A'*<sub>1</sub> mode is very sensitive to the doping of MoS<sub>2</sub>.<sup>[37]</sup> High concentration of sulfur vacancies and cracked regions are very active centers for molecular adsorption and, for example, adsorbed O<sub>2</sub> and/or H<sub>2</sub>O can introduce hole doping and thus reduce the electron concentration.<sup>[37]</sup> As it was shown in refs. [19,38,39], the reduced electron concentration leads to a blue shift of the *A'*<sub>1</sub> peak compared with the peak position in exfoliated high quality monolayer. It was also shown that the nitrogen doping could be an effective way to produce hole doping in MoS<sub>2</sub> monolayers<sup>[40]</sup> by creating N<sub>S</sub> acceptor defects. The presence of weak side peaks at about 409 and 378 cm<sup>-1</sup> (see **Figure 1(b)**) also confirms a high defect concentration in our monolayer, because these peaks were previously assigned to the defect-induced modes.<sup>[41,42]</sup>

Room temperature PL spectra of our MoS<sub>2</sub> show a clear presence of *A* and *B* bands at about 1.79 and 1.95 eV, respectively, see **Figure 2**. Additional weak band *X<sub>D</sub>* at 1.69 eV is also visible and it is related to defect bound excitons.<sup>[43]</sup> The relative PL intensity of the *B*-band was higher than usually observed in high quality MoS<sub>2</sub> monolayers and the overall photoluminescence intensity was also rather weak. In addition, we noticed a faint continuous background emission and it was subtracted during further analysis. All PL bands are red-shifted with respect to peak positions of high quality exfoliated monolayers and this is typical for CVD grown strained MoS<sub>2</sub> on SiO<sub>2</sub>/Si substrates.<sup>[19,44]</sup> At the same time, we did not observe any features corresponding to indirect transition usually visible in multilayers at about 1.5 eV.<sup>[45]</sup> This fact confirms that the red-shift of PL bands is caused by strained and defective MoS<sub>2</sub> monolayer and not by a presence of multilayers. The effect of tensile strain on PL properties of MoS<sub>2</sub> monolayers is studied in many papers and it was found that the decrease in the optical band gap is approximately linear with strain,  $\approx 45 \text{ meV}$  per % of strain for monolayer MoS<sub>2</sub>.<sup>[46]</sup>

Later studies showed even higher values,  $\approx 100 \text{ meV}$  per % of strain.<sup>[19,36,47]</sup> The peak position of the *A*-band in exfoliated MoS<sub>2</sub> monolayers is about 1.85 eV<sup>[48]</sup> and therefore we can expect to have  $\approx 0.6\%$  of strain in our monolayer. This strain is smaller than the estimated strain value from Raman measurements and therefore we expect that the shift of Raman peaks is partly caused also by charge doping.

The increase of an excitation intensity leads to nearly linear increase of the *A*-band intensity while the *B*-band shows a super-linear increase. Moreover, we noticed a red-shift of the *B*-band with increasing laser power, but the shape and the peak position of the *A*-band did not change. All these facts confirm that the *A*-band does not contain additional trion emission and we observe only emission of neutral excitons *A*<sup>0</sup>. At the same time, the behavior of the *B*-band can be explained if both trions and neutral excitons

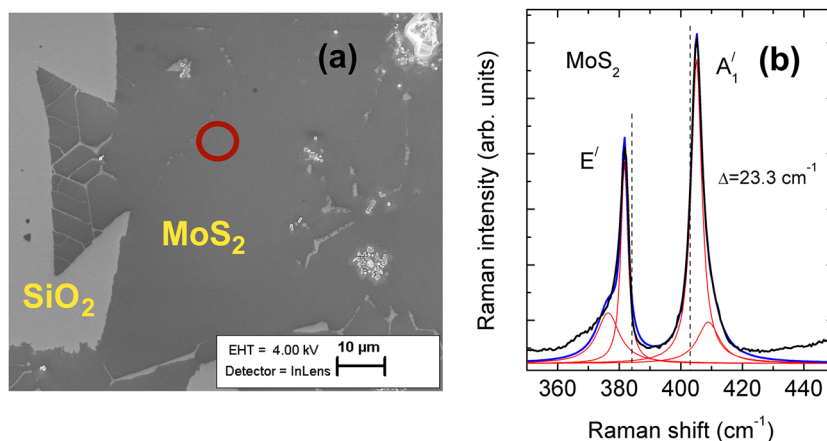


**Figure 1.** a) SEM picture of our MoS<sub>2</sub> monolayer, red circle indicates the location where Raman and PL spectra were measured. b) Raman spectrum from the monolayer area of MoS<sub>2</sub>. Red lines show a result of spectral fitting with Lorentzian curves and blue line is a cumulative fitting result. Vertical dashed lines represent the peak positions measured from high quality exfoliated MoS<sub>2</sub> monolayers.<sup>[32]</sup>

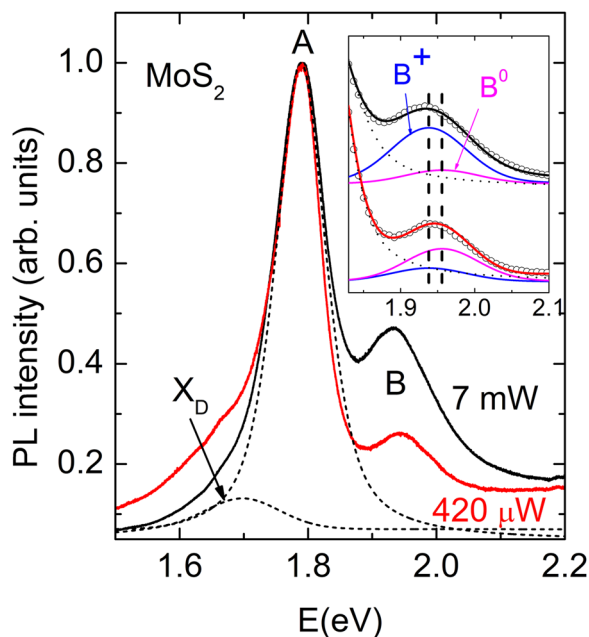


**Figure 2.** Normalized room temperature PL spectra of MoS<sub>2</sub> monolayer measured at different laser power. The inset shows a magnified range of the B-band with fitting results using pseudo-Voigt peak shape function for exciton (B<sup>0</sup>) (magenta line) and trion (B<sup>+</sup>) (blue line) and A-band (dotted curve). Experimental points are presented as circles, fitting results are given with solid black and red lines. Peak positions of B<sup>0</sup> and B<sup>+</sup> are marked with dashed vertical lines. Fitting result for the A-band (at 7 mW) is also shown as dashed lines.

are present. Different properties of A and B bands in our monolayer indicate that electrons in the conduction band play a minor role and holes in both valence bands determine emission properties. Therefore we probably have positive B-trions (B<sup>+</sup>) where two holes are paired with one electron. Accordingly, all PL spectra were fitted using a pseudo-Voigt line shapes for A<sup>0</sup>, B<sup>+</sup>, and B<sup>0</sup>. The separation between our B<sup>0</sup> and B<sup>+</sup> bands was found to be 18 meV and it was kept constant in all fittings. Based on deterioration of the fit upon changing this separation, we estimate the uncertainty of the trion binding energy to be less than 2 meV. By changing the laser excitation intensity over a factor of 150, the peak positions and peak widths (FWHM) of these PL bands did not change indicating no heating of the sample over the range of laser powers used. An example of this fitting for the B band region is shown in Figure 2. At lower laser powers, the B<sup>0</sup> band dominates at 1.956 eV but at higher laser powers we clearly see a rapid increase of the B<sup>+</sup> band at 1.938 eV. The value of spin orbit splitting in our monolayer is found to be  $\Delta E_{SO} = 166$  meV and it is slightly bigger than in high quality monolayers. According to recent first-principles calculations,<sup>[29]</sup> the binding energy of trions in MoS<sub>2</sub> monolayers somewhat depends on substrate and for SiO<sub>2</sub>/Si substrate values 35/32 and 18/17 meV were found for A<sup>-</sup>/A<sup>+</sup> and B<sup>-</sup>/B<sup>+</sup> trions, respectively. The latter agrees very well with our experimental value. Very small binding energy for the B trion explains why it is so difficult to resolve B trion emission while A trion is often visible even at room temperature.

In general, the excitation intensity dependence of the PL intensity is a good indicator of the nature of radiative recombination processes. Specifically, the integral PL intensity,  $I$ , shows a power law dependence on the laser excitation power,  $P$ , as  $I \sim P^k$ . A value of  $k \approx 1$  indicates an exciton-like transition and  $k \ll 1$  suggests a recombination path involving defects.<sup>[49]</sup> For trions, where the recombination involves three particles, the intensity should show a  $P^{1.5}$  dependence, i.e., superlinear increase on laser power.<sup>[14]</sup> If both trion and neutral excitons are present, then the increase of B-band intensity must have superlinear dependence with  $1 < k < 1.5$ . The actual value of  $k$  for each PL band depends also on other conditions like type of a substrate, defect concentration, and crystal quality of monolayers. The dependence of integral intensity of PL bands on laser power is presented in Figure 3. Both neutral excitons (A<sup>0</sup>, B<sup>0</sup>) show nearly linear increase with laser power (note that the B<sup>0</sup>-band seems to have almost the same behavior as the A<sup>0</sup>-band at higher laser power), but the B<sup>+</sup> band increases with  $k = 1.42$ . This value correlates with the expected value for trions ( $k = 1.5$ ). The total intensity of the B-band increases with laser power as  $I \sim P^{1.25}$ .

All properties of our MoS<sub>2</sub> monolayer indicate that we have a very high concentration of defects and quite low carrier concentration. The reason for the fairly intense B-band emission, as compared to those reported in the literature, is therefore assigned to defects. In particular, we assume that there is a non-radiative recombination channel that preferentially acts on the holes in the A-band. This can occur if the traps are energetically close to the valence band maximum, which is responsible for the A-band emission. For example, as it was shown in ref. [50], sulfur adatoms on the surface of MoS<sub>2</sub> layer can introduce a very fast non-radiative recombination channel.

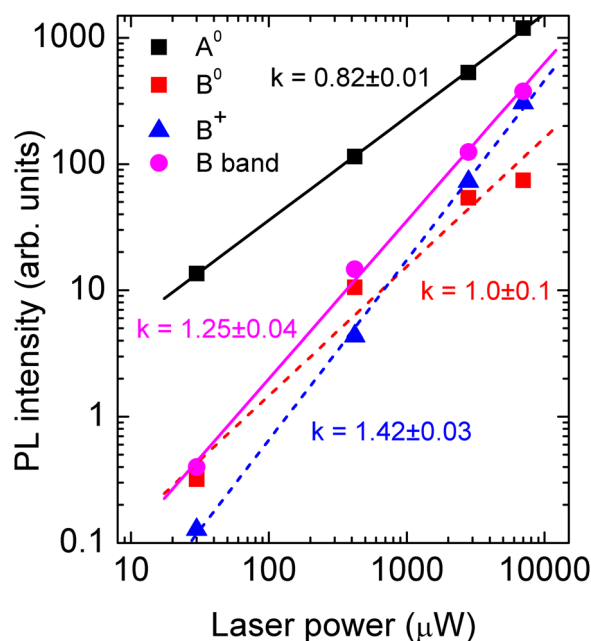


**Figure 3.** Integrated photoluminescence intensity of different PL bands as a function of the laser power plotted on a log–log scale. The lines are least squares fit to the data.

The difference in the relative intensities of trions and excitons in the *A* and *B* bands also appears puzzling. After all, the presence of *B*-trions should imply the presence of free carriers and thereby also of *A*-trions. We speculate on two scenarios for this apparent discrepancy: either the density of *A*-trions or their emission intensity is suppressed. For the former, if there is fast recombination channel for the *A*-excitons, as also assumed above, they will recombine before they can find free carrier and thereby form a trion. Thus, the *A*-trion formation is suppressed. In this scenario, it is irrelevant whether the free carriers are electrons or holes, as long as their concentration is low. The fast recombination channel does not need to be completely non-radiative, but it needs to be selective to *A* to keep the exciton density sufficiently low, while *B*-excitons live longer and form trions. In the latter scenario, the calculated lowest energy  $B^+$  trion has one hole in the highest valence band (VB) and one hole in the lower spin-orbit-split band (VB-1). This could in principle show up either as  $A^+$  trion or as  $B^+$  trion. However, due to the spin orientation in the relevant bands, it is expected to be dark in *A*, but bright in *B*,<sup>[29,51]</sup> and thus shows up more strongly as  $B^+$ . The reason for the enhancement of this type of trions over “normal”  $A^+$  trions could be ascribed to the same process as in the previous scenario. Alternatively, we could assume there is a fast non-radiative recombination mechanism that affects similarly both conduction band states, but preferentially the VB holes over the VB-1 holes. Then, *B*-exciton is broken via electron trapping and subsequently recombines with VB hole, but a hole is left in the VB-1 state. Since the hole concentration is subsequently reduced at VB state, this essentially leads to transferring the hole concentration from

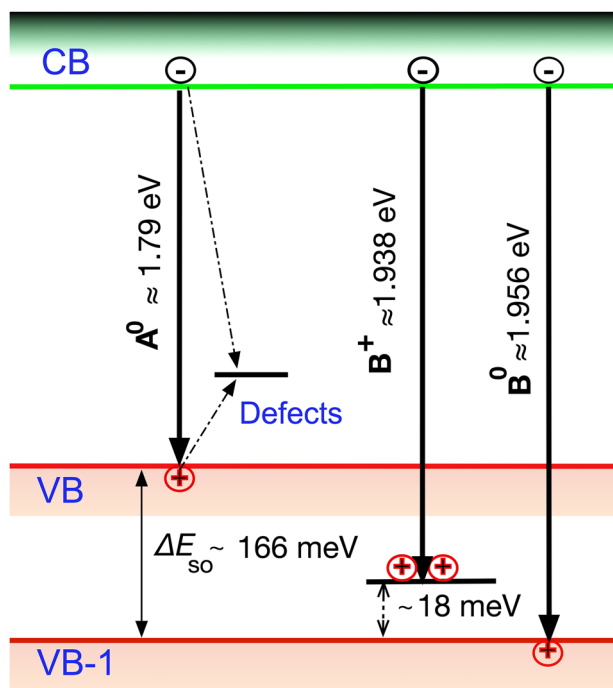


**Figure 4.** The band structure near the *K*-point of the Brillouin zone showing radiative and non-radiative emissions in MoS<sub>2</sub> monolayer.

VB to VB-1. Consequently the trion can be formed even as combination of *A*-exciton and hole at VB-1.

The band structure with all the observed emissions are summarized in **Figure 4**. Following the above discussion, we have also illustrated the possible defect-induced recombination channel in the figure, although at present the exact nature of the defects remains unknown. Also further studies are needed to investigate the properties of *B*-trions in more detail.

## 4. Conclusions

Photoluminescence spectra of our CVD grown MoS<sub>2</sub> monolayer exhibit two predominant bands (*A* and *B*) corresponding to the optical transitions at the *K*-point in the Brillouin zone. High concentration of defects in our sample creates a fast non-radiative recombination channel and additionally reduces a carrier concentration.

While the *A*-band exhibits only specific excitonic properties, the *B*-band has a double structure. The evolution of the *B*-band shape upon variable excitation power is well described by a combination of exciton and trion contributions, from which we extract *B*-trion binding energy of 18 meV.

## Acknowledgments

This work was supported by institutional research funding IUT (IUT19-28) of the Estonian Ministry of Education and Research, by the European Union through the European Regional Development Fund, Project TK141, and the Academy of Finland through project No. 311058. The authors acknowledge fruitful discussion with Dr. Thorsten Deilmann.

## Conflict of Interest

The authors declare no conflict of interest.

## Keywords

chemical vapor deposition, monolayers, MoS<sub>2</sub>, photoluminescence, trions

Received: July 25, 2018

Revised: September 24, 2018

Published online:

- [1] K. S. Novoselov, D. Jiang, F. Schedin, T. J. Booth, V. V. Khotkevich, S. V. Morozov, A. K. Geim, *Proc. Natl. Acad. Sci. USA* **2005**, *102*, 10451.
- [2] J. Xiao, M. Zhao, Y. Wang, X. Zhang, *Nanophotonics* **2017**, *6*, 1309.
- [3] K. F. Mak, C. Lee, J. Hone, J. Shan, T. F. Heinz, *Phys. Rev. Lett.* **2010**, *105*, 2.
- [4] Y. P. Venkata Subbaiah, K. J. Saji, A. Tiwari, *Adv. Funct. Mater.* **2016**, *26*, 2046.
- [5] Y.-H. Lee, X.-Q. Zhang, W. Zhang, M.-T. Chang, C.-T. Lin, K.-D. Chang, Y.-C. Yu, J. T.-W. Wang, C.-S. Chang, L.-J. Li, T.-W. Lin, *Adv. Mater.* **2012**, *24*, 2320.
- [6] J. Krustok, T. Raadik, R. Jaaniso, V. Kiisk, I. Sildos, M. Marandi, H.-P. Komsa, B. Li, X. Zhang, Y. Gong, P. M. Ajayan, *Appl. Phys. Lett.* **2016**, *109*, 253106.

- [7] N. Kosku Perkgöz, *Anadolu Univ. J. Sci. Technol. A – Appl. Sci. Eng.* **2017**, *18*, 375.
- [8] J. Xia, X. Huang, L.-Z. Liu, M. Wang, L. Wang, B. Huang, D.-D. Zhu, J.-J. Li, C.-Z. Gu, X.-M. Meng, *Nanoscale* **2014**, *6*, 8949.
- [9] A. Özden, F. Ay, C. Sevik, N. K. Perkgöz, *Jpn. J. Appl. Phys.* **2017**, *56*, 06GG05.
- [10] H. Bergeron, V. K. Sangwan, J. J. McMorro, G. P. Campbell, I. Balla, X. Liu, M. J. Bedzyk, T. J. Marks, M. C. Hersam, *Appl. Phys. Lett.* **2017**, *110*, 53101.
- [11] J. Krustok, R. Kaupmees, R. Jaaniso, V. Kiisk, I. Sildos, B. Li, Y. Gong, *AIP Adv.* **2017**, *7*, 65005.
- [12] X. Wang, H. Feng, Y. Wu, L. Jiao, *J. Am. Chem. Soc.* **2013**, *135*, 5304.
- [13] A. Splendiani, L. Sun, Y. Zhang, T. Li, J. Kim, C. Y. Chim, G. Galli, F. Wang, *Nano Lett.* **2010**, *10*, 1271.
- [14] D. Kaplan, Y. Gong, K. Mills, V. Swaminathan, P. M. Ajayan, S. Shirodkar, E. Kaxiras, *2D Mater.* **2016**, *3*, 15005.
- [15] K. P. Dhakal, D. L. Duong, J. Lee, H. Nam, M. Kim, M. Kan, Y. H. Lee, J. Kim, *Nanoscale* **2014**, *6*, 13028.
- [16] G.-B. Liu, W.-Y. Shan, Y. Yao, W. Yao, D. Xiao, *Phys. Rev. B* **2013**, *88*, 85433.
- [17] G. Plechinger, J. Mann, E. Preciado, D. Barroso, A. Nguyen, J. Eroms, C. Schüller, L. Bartels, T. Korn, *Semicond. Sci. Technol.* **2014**, *29*, 064008.
- [18] C. R. Zhu, G. Wang, B. L. Liu, X. Marie, X. F. Qiao, X. Zhang, X. X. Wu, H. Fan, P. H. Tan, T. Amand, B. Urbaszek, *Phys. Rev. B* **2013**, *88*, 121301(R).
- [19] W. H. Chae, J. D. Cain, E. D. Hanson, A. A. Murthy, V. P. Dravid, *Appl. Phys. Lett.* **2017**, *111*, 143106.
- [20] R. Roldán, A. Castellanos-Gomez, E. Cappelluti, F. Guinea, *J. Phys.: Condens. Matter* **2015**, *27*, 313201.
- [21] W. M. Parkin, A. Balan, L. Liang, P. M. Das, M. Lamparski, C. H. Naylor, J. A. Rodríguez-Manzo, A. T. C. Johnson, V. Meunier, M. Drndić, *ACS Nano* **2016**, *10*, 4134.
- [22] C. Rice, R. J. Young, R. Zan, U. Bangert, D. Wolverson, T. Georgiou, R. Jalil, K. S. Novoselov, *Phys. Rev. B* **2013**, *87*, 81307.
- [23] Y. Wang, C. Cong, C. Qiu, T. Yu, *Small* **2013**, *9*, 2857.
- [24] K. F. Mak, K. He, C. Lee, G. H. Lee, J. Hone, T. F. Heinz, J. Shan, *Nature Mater.* **2012**, *12*, 207.
- [25] Y. Lin, X. Ling, L. Yu, S. Huang, A. L. Hsu, Y.-H. Lee, J. Kong, M. S. Dresselhaus, T. Palacios, *Nano Lett.* **2014**, *14*, 5569.
- [26] J. W. Christopher, B. B. Goldberg, A. K. Swan, *Sci. Rep.* **2017**, *7*, 14062.
- [27] M. D. Tran, J. H. Kim, Y. H. Lee, *Curr. Appl. Phys.* **2016**, *16*, 1159.
- [28] T. C. Berkelbach, M. S. Hybertsen, D. R. Reichman, *Phys. Rev. B* **2013**, *88*, 45318.
- [29] M. Drüppel, T. Deilmann, P. Krüger, M. Rohlfiing, *Nature Commun.* **2017**, *8*, 2117.
- [30] I. Kylänpää, H.-P. Komsa, *Phys. Rev. B* **2015**, *92*, 205418.
- [31] Z. Wang, L. Zhao, K. F. Mak, J. Shan, *Nano Lett.* **2017**, *17*, 740.
- [32] X. Li, H. Zhu, *J. Mater.* **2015**, *7*, 33.
- [33] C. Lee, H. Yan, L. E. Brus, T. F. Heinz, J. Hone, S. Ryu, *ACS Nano* **2010**, *4*, 2695.
- [34] H. Li, Q. Zhang, C. C. R. Yap, B. K. Tay, T. H. T. Edwin, A. Olivier, D. Baillargeat, *Adv. Funct. Mater.* **2012**, *22*, 1385.
- [35] A. Michail, N. Delikoukos, J. Parthenios, C. Galiotis, K. Papagelis, *Appl. Phys. Lett.* **2016**, *108*, 173102.
- [36] H. Li, A. W. Contryman, X. Qian, S. M. Ardakani, Y. Gong, X. Wang, J. M. Weisse, C. H. Lee, J. Zhao, P. M. Ajayan, J. Li, H. C. Manoharan, X. Zheng, *Nature Commun.* **2015**, *6*, 7381.
- [37] H. Nan, Z. Wang, W. Wang, Z. Liang, Y. Lu, Q. Chen, D. He, P. Tan, F. Miao, X. Wang, J. Wang, Z. Ni, *ACS Nano* **2014**, *8*, 5738.
- [38] B. Chakraborty, A. Bera, D. V. S. Muthu, S. Bhowmick, U. V. Waghmare, A. K. Sood, *Phys. Rev. B* **2012**, *85*, 161403.
- [39] A. Bera, D. V. S. Muthu, A. K. Sood, *J. Raman Spectrosc.* **2018**, *49*, 100.
- [40] A. Azcatl, X. Qin, A. Prakash, C. Zhang, L. Cheng, Q. Wang, N. Lu, M. J. Kim, J. Kim, K. Cho, R. Addou, C. L. Hinkle, J. Appenzeller, R. M. Wallace, *Nano Lett.* **2016**, *16*, 5437.
- [41] S. Mignuzzi, A. J. Pollard, N. Bonini, B. Brennan, I. S. Gilmore, M. A. Pimenta, D. Richards, D. Roy, *Phys. Rev. B* **2015**, *91*, 195411.
- [42] D. Wu, H. Huang, X. Zhu, Y. He, Q. Xie, X. Chen, X. Zheng, H. Duan, Y. Gao, *Crystals* **2016**, *6*, 151.
- [43] A. Zafar, H. Nan, Z. Zafar, Z. Wu, J. Jiang, Y. You, Z. Ni, *Nano Res.* **2017**, *10*, 1608.
- [44] Z. Liu, M. Amani, S. Najmaei, Q. Xu, X. Zou, W. Zhou, T. Yu, C. Qiu, A. G. Birdwell, F. J. Crowne, R. Vajtai, B. I. Yakobson, Z. Xia, M. Dubey, P. M. Ajayan, J. Lou, *Nature Commun.* **2014**, *5*, 5246.
- [45] N. Scheuschner, O. Ochedowski, A.-M. Kaulitz, R. Gillen, M. Schleberger, J. Maultzsch, *Phys. Rev. B* **2014**, *89*, 125406.
- [46] H. J. Conley, B. Wang, J. I. Ziegler, R. F. Haglund, S. T. Pantelides, K. I. Bolotin, *Nano Lett.* **2013**, *13*, 3626.
- [47] D. Lloyd, X. Liu, J. W. Christopher, L. Cantley, A. Wadehra, B. L. Kim, B. B. Goldberg, A. K. Swan, J. S. Bunch, *Nano Lett.* **2016**, *16*, 5836.
- [48] Z. Li, S.-W. Chang, C.-C. Chen, S. B. Cronin, *Nano Res.* **2014**, *7*, 973.
- [49] T. Schmidt, K. Lischka, *Phys. Rev. B* **1992**, *45*, 8989.
- [50] L. Li, R. Long, T. Bertolini, O. V. Prezhdo, *Nano Lett.* **2017**, *17*, 7962.
- [51] T. Deilmann, K. S. Thygesen, *Phys. Rev. B* **2017**, *96*, 201113.